The Coma of Comet 2P/Encke

Paul D. Feldman (pdf@pha.jhu.edu)
Department of Physics and Astronomy, The Johns Hopkins University, Charles and 34th Streets, Baltimore, Maryland 21218

Anita L. Cochran (anita@barolo.as.utexas.edu)
The University of Texas McDonald Observatory, Austin, Texas 78712

Andrew F. Cheng (andy.cheng@jhuapl.edu)
The Johns Hopkins Applied Physics Laboratory, 11100 Johns Hopkins Road, Laurel Maryland 20723

Michael J. S. Belton (belton@azstarnet.com)
Belton Space Exploration Initiatives, LLC, 430 S. Randolph Way, Tucson, Arizona 85716

Abstract.

Space and ground-based observations of comet 2P/Encke made during the past thirty years together with recent modeling have provided a qualitative understanding of the nature and temporal evolution of the gaseous coma of the comet. Details of the interface between coma and nucleus remain obscure. In this context we outline the objectives and approach of the CONTOUR coma imaging investigation.

1. Introduction

Periodic comet 2P/Encke, the first comet to be visited by CONTOUR, is perhaps the most studied comet of recent times (for an excellent historical review see Sekanina (1991b) as well as the paper by Yeomans and Belton in this volume). Its short period (3.3 yr) and relatively stable orbit provided ample opportunity to measure the effects of "non-gravitational" forces on its orbit, the analysis of which in terms of asymmetric outgassing of the nucleus, played a pivotal role in the development of the dirty ice conglomerate model of the comet nucleus by Whipple (1950). The importance of water ice in the nucleus was subsequently confirmed by observations from above the terrestrial atmosphere of the dissociation products, H (Bertaux et al., 1973) and OH. Measurements of H I Lyman-α at 1216 Å and OH fluorescence at 3085 Å have continued to provide information about the water production rates of many comets, both short-period comets such as Encke, as well as for comets entering the inner solar system for the first time. These are supplemented by radio observations of OH at 18 cm, spectroscopy and narrow-band imaging of O I $^1D - ^3P$ emission at 6300 and 6364 Å, oxygen atoms in the ^1D state being another water dissociation product, and, more recently, direct observations of H_2O in the infrared, in many cases providing long term monitoring of the evolution of cometary activity over an entire apparition. However, at the spatial resolution of even the best current ground or space-based telescopes, the details of the mechanisms by which gas and dust are released from the nucleus remain obscure. Evidence from the spacecraft fly-bys of periodic comets Halley and Borrelly and from observations of other recent comets suggests that only a small fraction (10–20%) of the sunlit surface of a comet nucleus is active, with periodic comets having much smaller active areas than long-period dynamically new comets (Sekanina, 1991a). Imaging of the gas and dust close to the nucleus in order to elucidate these mechanisms is the principal objective of the CONTOUR coma imaging investigation.

The CONTOUR Forward Imager (CFI) has the capability to obtain spectral images of gas emission using narrow band filters. Our focus will be on OH fluorescence in the $A\,^2\Sigma^+ - X\,^2\Pi$ (0,0) band at 3085 Å as a measure of H_2O outgassing and monitoring of CN (3883 Å) and C_2 (4850 Å) emission associated with dust jets. Near the nucleus (within 50–100 km, depending on the heliocentric velocity of the comet), prompt emission of the OH (0,0) band from dissociative excitation of H_2O by solar extreme ultraviolet radiation dominates fluorescence and provides a direct tracer for H_2O escaping from the nucleus (Bertaux, 1986; Budzien and Feldman, 1991).

2. The Gas Coma of Comet 2P/Encke

The visible coma of comet Encke (*e.g.*, Djorgovski and Spinrad (1985)) shows a strong sunward fan that is attributed to localized outgassing from the nucleus (Festou and Barale, 2000). Except very close to the nucleus, the images of the optical fan do not contain much reflected sunlight from micron-sized grains, but rather gas emissions at the wavelengths of the C_2, C_3, and CN radicals. In this case, the visual light curve can be related directly to the production rates of these minor species. OH similarly displays an asymmetric coma (Feldman et al., 1984) which Festou and Barale have modeled with the same geometry as for the optical fan. However, they caution that the H_2O production rate that they derive is $\sim 30\%$ lower than earlier published values based on spherically symmetric models. A visible image taken in November 1980 by S. M. Larson (from Feldman et al. (1984)) is shown in Figure 1. The aysmmetric distribution of the gas and dust in Encke's coma is strikingly illustrated by spatial profiles derived from long-slit spectroscopy shown in Figure 2.

2.1. Water Production

In this section we shall review some of the indirect measurements of the water production rate of comet Encke made over the past thirty years. While the OH $A\,^2\Sigma^+ - X\,^2\Pi$ (0,0) band at 3085 Å had been observed in many comets, because its wavelength lies close to the atmospheric cut-off and comets are usually observed at large airmass, it was not until the first cometary observations by the *Orbiting Astronomical Observatory-2* in 1969 and 1970 that the strength of this emission was appreciated (Code et al., 1972). At the same time, the very extended H I Lyman-α halo associated with fast hydrogen atoms produced by the photodissociation of H_2O and OH and interacting with the solar wind was also discovered. The launch of the *International Ultraviolet Explorer* (*IUE*) in January 1978 and its operation in geosynchronous orbit until late 1996 provided a stable, well-calibrated platform above the atmosphere for the observation of these emissions in nearly 50 comets, some, such as Encke, over multiple apparitions. Encke was observed by *IUE* in 1980, 1990, and 1993 pre-perihelion, and in 1984 and 1987 post-perihelion. The most extensive set of measurements was made during October–November 1980 when the viewing geometry was particularly favorable (the initial solar avoidance constraint of *IUE* was 45°), and this set included mapping of the OH emissions (Feldman et al., 1984; Festou and Barale, 2000) and high-dispersion spectroscopy of the (0,0) band sunward and tailward in order to determine the non-gravitational parameters using the Swings effect (A'Hearn and Schleicher, 1988). An attempt to ascertain the secular decrease of water production rate with time over the five apparitions was made by M. Haken

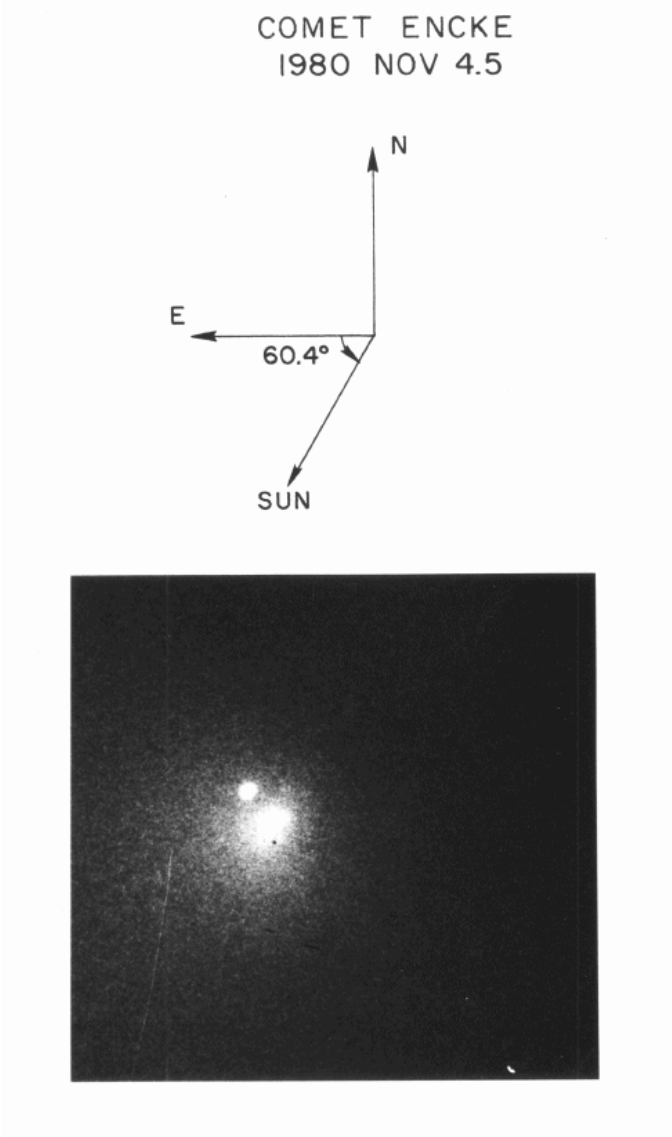

Figure 1. Visible image of comet Encke taken by S. M. Larson on November 4, 1980. A star is located just northeast of the location of the comet's nucleus. From Feldman et al. (1984).

et al. (unpublished manuscript), but uncertainties in the pointing during the 1990 and 1993 apparitions made the results ambiguous.

A composite *IUE* spectrum taken November 4, 1980 is shown in Figure 3. The data are the same as shown by Feldman et al. (1984) but have been reprocessed for the *IUE* archive using the *NEWSIPS* package. A long and short exposure is used for both wavelength ranges with the gray lines repre-

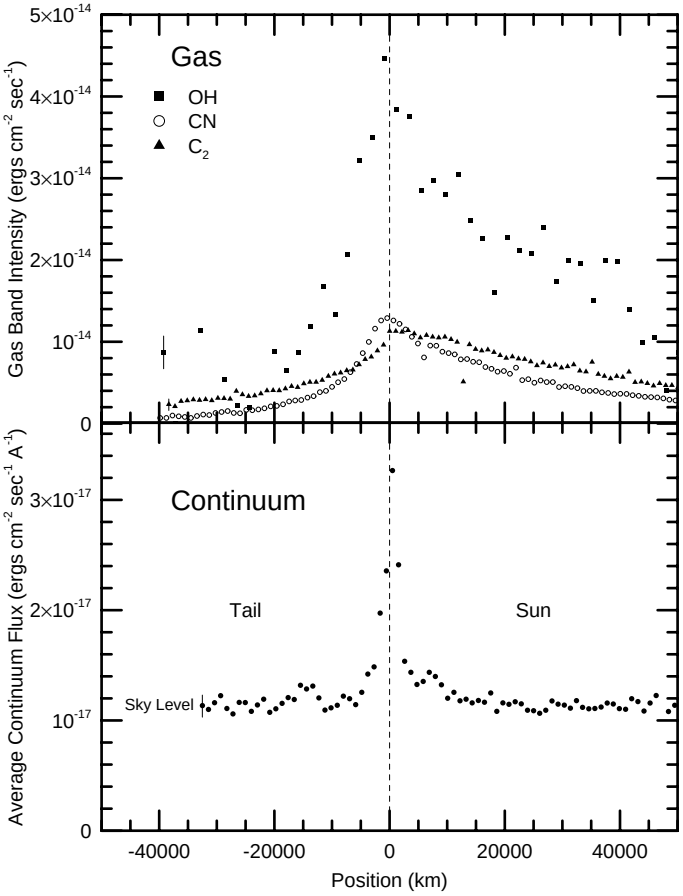

Figure 2. The band intensity of the gas and the average continuum flux were measured on 28 August 1990 with a long slit CCD spectrograph at McDonald Observatory. The mentioned asymmetries are quite apparent for the three gas species though the degree of asymmetry is different for different molecules. Note that the dust is confined to the very inner coma. Representative error bars are included on the left-most data point for each species except CN, where the error bars are the size of the points.

senting the brightness divided by 500 in the top spectrum and by 20 in the bottom panel. Note the dominance of the emissions of H and OH, but also the presence of resonance emissions of atomic carbon, oxygen, and sulfur, and the molecule CS, all routinely seen in comets in this spectral range. The continuum near 3000 Å is barely detectable and is consistent with the very high gas/dust ratio deduced from optical spectroscopy and photometry.

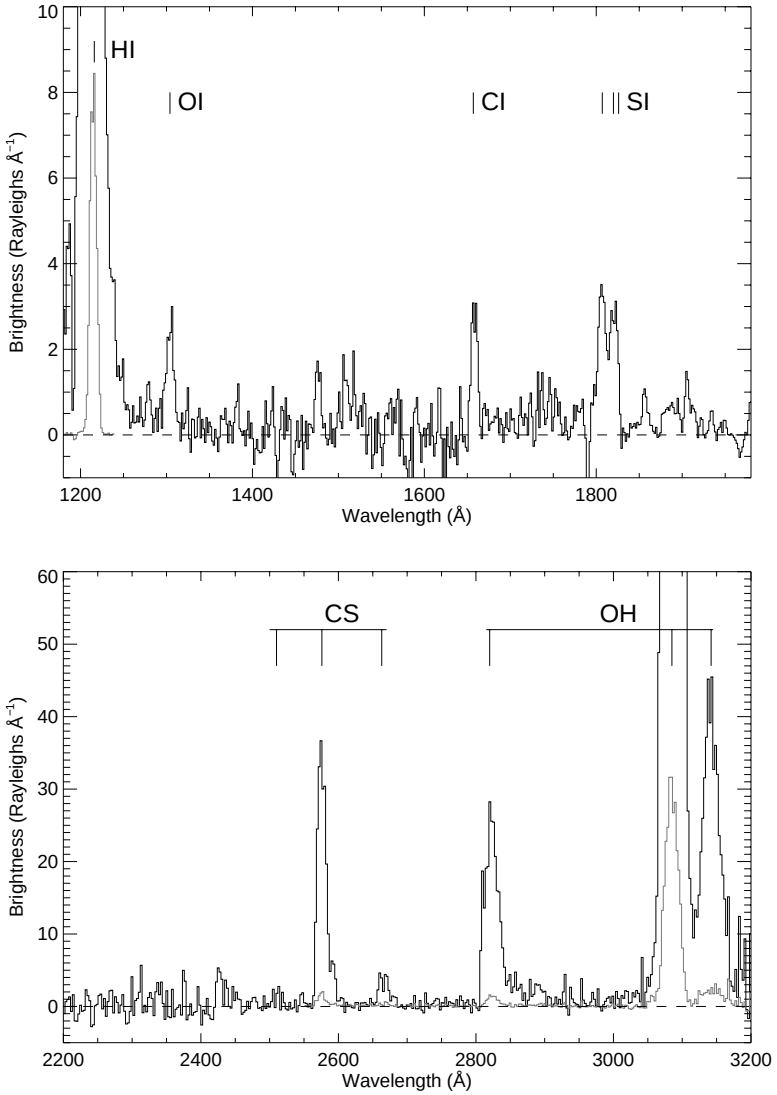

Figure 3. Composite *IUE* spectrum of comet 2P/Encke taken on November 4, 1980 from Feldman et al. (1984). Top: SWP10544 and SWP10548 (divided by 500; gray line). Bottom: LWR9232 and LWR9233 (divided by 20; gray line).

Water production rates are derived from these spectra by integrating the brightness in each OH band and by comparing this result to the predictions of a vectorial model (Festou, 1981) using photodissociation lifetimes and branching ratios appropriate to solar activity at the time (Budzien et al., 1994). Velocity dependent fluorescence efficiencies for the OH bands are taken from Schleicher and A'Hearn (1988). The results from the 1980 and 1984 appari-

tions are shown in Figure 4. From the *IUE* data alone we find, for heliocentric distance, r, greater than 0.75 AU, a variation in water production rate of $r^{-3.4}$ and no difference between pre-perihelion and post-perihelion. Also included in the figure is the result of the model of Festou and Barale (2000), showing a 30% decrease in water production rate relative to that derived from symmetric coma models.

This result is in strong contrast with the production rates derived from narrow-band photometry of C_2 and CN which show a post-perihelion decrease, at 0.8 AU, of a factor of $\sim$3.5 (A'Hearn et al., 1985). The *IUE* spectra provide additional evidence of this asymmetry about perihelion for the minor coma species. A'Hearn et al. also show an *IUE* spectrum from 1984 in which the CS emission is sharply reduced relative to the OH seen in Fig. 3. Using revised CS fluorescence efficiencies from R. Yelle (private communication), we find $Q_{CS_2}/Q_{H_2O} = 1.4 \times 10^{-3}$ at $r = 0.84$ AU pre-perihelion and 4.2×10^{-4} at $r = 0.76$ AU post-perihelion, a decrease of a factor of 3.3, commensurate with that seen in C_2 and CN. This result can be understood in terms of chemical heterogeneity between the two discrete outgassing vents identified by Sekanina (1988a) from dynamical analysis of the sunward fan, the two vents being active during either the inbound or outbound legs of the orbit but not both simultaneously. Fortuitously, CONTOUR will fly by Encke at $r = 1.07$ AU, 47 days before perihelion, allowing the mass spectrometer (NGIMS) to sample a higher concentration of minor species.

A'Hearn et al. (1985) also present ground-based OH observations made at four apparitions of Encke. In Fig. 4 their data from 1984, both pre- and post-perihelion, are shown, adjusted by a factor of two to convert from their use of a Haser model to the same parameters used above. In addition, they give Q_{OH} rather than Q_{H_2O}, which we scale by a factor of 1.1. Their data suggest a lessening of the slope for $r < 0.8$ AU with a particularly severe downturn pre-perihelion, similar to what they reported from pre-perihelion observations in 1980 (A'Hearn et al., 1983). The reality of the change in slope, though not relevant for the CONTOUR mission, can be addressed with recent H I Lyman-α observations of Encke made by two separate instruments on the *Solar and Heliospheric Observatory* (*SOHO*). The lower panel of Figure 4 shows water production rates derived from 1997 *SOHO*/SWAN data by Mäkinen et al. (2001) and from 2000 *SOHO*/UVCS spectra taken very close to perihelion by Raymond et al. (2002). For comparison with the upper panel, the dashed line with slope –3.4 is repeated and it is seen that the results of Mäkinen et al. for $r > 0.7$ AU give reasonably fair agreement to the post-perihelion OH data. Unfortunately there is a gap in the SWAN data between $\sim$0.4 and 0.7 AU caused by contamination from the very bright Lyman-α coma of comet C/1995 O1 (Hale-Bopp) which was present in the sky at the same time. Despite the unexplained discrepancy of a factor of $\sim$2.5 between the near-perihelion results of Mäkinen et al. and those of Raymond et al., it is

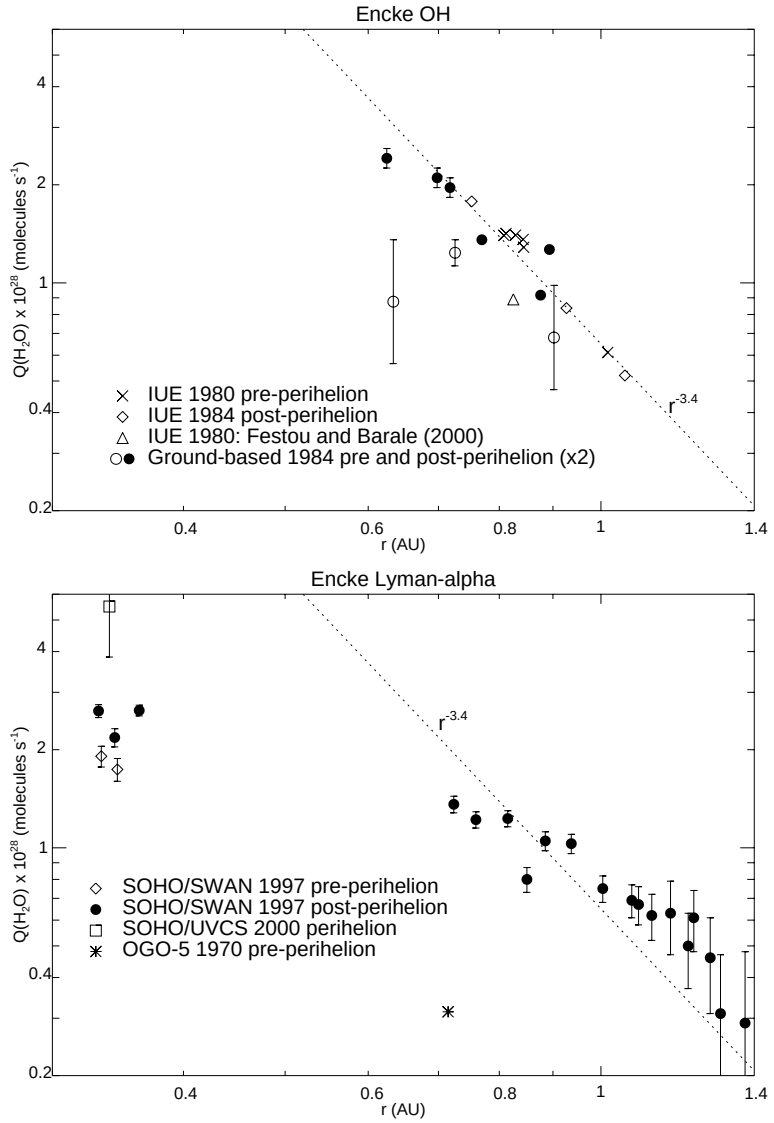

Figure 4. Water production rate of comet 2P/Encke as derived from observations of OH (top) and H I Lyman-α (bottom). Error bars are shown when given with the original data.

clear that there is a significant change in slope of Q_{H_2O} for $r < 0.75$ AU, and that at perihelion the water production rate of Encke reaches a maximum of $\sim 5 \times 10^{28}$ molecules s^{-1}. Raymond et al. also claim to see a 30% increase in Lyman-α brightness two days after perihelion which they attribute to the activation of the second vent, in accordance with the predictions of the model of Sekanina (1988a).

Sanzovo et al. (2001) have recently derived gas release rates for comet Encke and several other comets using an empirically derived relationship between Q_{H_2O} and visual magnitude in a fixed aperture. Their results are in complete discord with those presented above, as they find a strong asymmetry about perihelion and a peak water production rate at perihelion of $\sim 2 \times 10^{29}$ molecules s^{-1}. Their asymmetry is probably the result of the assumptions of their method which do not fit well with comet Encke since the visual magnitudes of Encke are so strongly influenced by the lack of dust in the coma.

2.2. CN AND C_2

The optical spectrum of a comet is dominated by bands of molecular radicals, with CN, C_2 and C_3 being the strongest. Figure 5 shows the spectrum of comet Encke when the comet was at 1.3 AU, a distance slightly further from the Sun than the CONTOUR encounter distance. Shown in this figure are a spectrum from the optocenter and one from almost 16,000 km away. These spectra have had the background sky spectrum removed but no reflected solar spectrum has been removed. Despite this, there is almost no continuum observed.

The lack of a continuum indicates that the coma of Encke is depleted in small dust particles. This is in accord with the findings of Sekanina and Schuster (1978) and Reach et al. (2000). Indeed, Reach et al. found evidence for long-lived particles of size $\sim$5 cm with data from the Infrared Space Observatory, but conclude there is no evidence of a "classical" cometary dust tail with small particles.

Comparison of the upper and lower panels of Figure 5 shows that the molecular band strengths decrease with distance from the nucleus but the decrease is much stronger for C_3 than for C_2 or CN. A'Hearn et al. (1995) have shown that Encke produces CN, C_2 and C_3 in "normal" proportions relative to OH. This is true despite the fact that the comet has been in the inner Solar System for an extremely long time and that it has one of the highest gas-to-dust ratios of any comet.

2.3. THE SUNWARD FAN AND ITS SOURCE REGIONS

Encke's visible coma, as has been mentioned above, usually contains a diffuse structure referred to as a fan that emanates on the sunward side of the nucleus. Its dimensions are such that it stretches typically $\sim 10^5$ km on the sunward side of the nucleus (but not necessarily directly towards the sun) with a included angle of 80 to 120°. There are no well-defined features in photographs of this structure, although early visual observers sometimes drew enhanced brightness along its outer edges. The projected geometry of this fan, which appears to be defined by molecular emissions, has been found

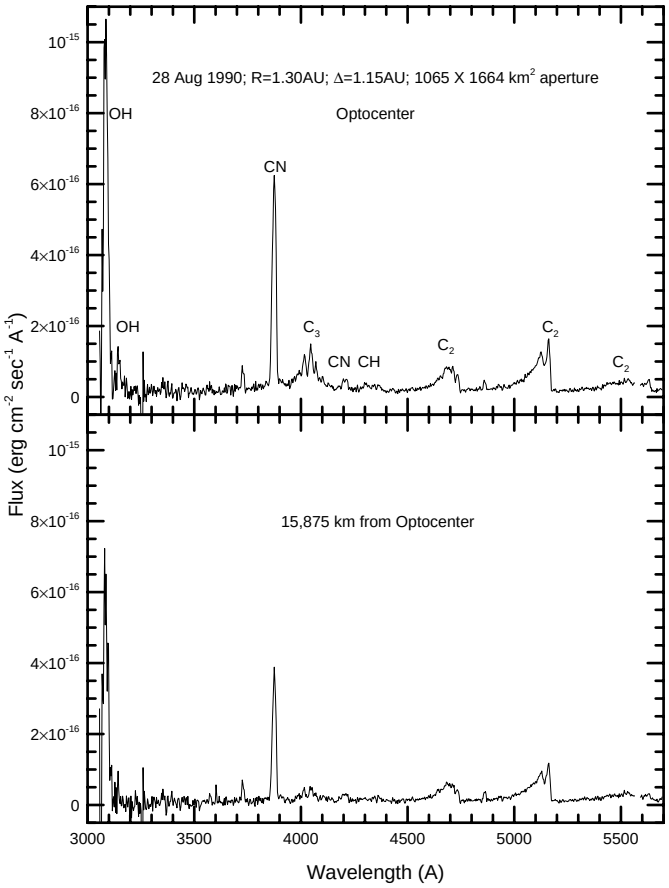

Figure 5. The visible spectrum of Encke's optocenter and a region of the coma 15,875 km away are shown. These spectra were obtained with a long-slit CCD spectrograph at McDonald Observatory. The sky spectrum has been subtracted but no solar spectrum has been removed. Note the lack of any continuum in these spectra, as well as the relative decrease of the various species.

to change in a systematic way, sometimes disappearing altogether to present an essentially circularly symmetric coma, depending on the position of the comet in orbit and the Earth viewing geometry. This phenomenon has been studied in detail by Sekanina (1988a; 1988b) who provides an interpretation that is based on a rotating nucleus, with a fully relaxed spin state, with two well defined active areas, one in the north at $\sim 55^\circ$ latitude and the other near -75° in the south. With the polar axis oriented towards $\alpha = 205^\circ$, $\delta = +2^\circ$ (1950) at the present epoch, not far from the pole later deduced by Festou and

Barale (2000), Sekanina invokes a narrowly collimated outflow (at least for dust entrained close to the nucleus) from the illuminated active area which forms, as a result of rotation, a diffuse conical sheet of material, with half angle of $\sim 35^\circ$, escaping from the nucleus that is roughly symmetric around the polar axis. With this geometry, and when viewed from the Earth with the line of sight outside of the cone, a fan shaped structure with the observed half angle and orientation should be seen. At those times when the line of sight from the earth is well within the conical surface the fan disappears to resolve itself into a more normal coma with roughly circular symmetry.

The CONTOUR mission gives an excellent opportunity to test these ideas. The spacecraft will approach Encke's nucleus over its northern hemisphere at a time when Sekanina's rotation pole is $\sim 30^\circ$ from the sunline and $\sim 40^\circ$ from the trajectory approach vector (the angle between the sunline and the approach vector is small at 12°). This means that Sekanina's active area at 55° latitude will be illuminated at encounter and the line of sight (and trajectory) will traverse the coma just on the outside edge of the emission cone. If the fully relaxed spin assumed by Sekanina is borne out, the long axis of the elongated nucleus should be tilted by less than 40° from the image plane providing excellent viewing of the nucleus just before encounter.

3. Observations of Coma Emissions with CONTOUR

The CONTOUR encounter with comet Encke will occur at 1.07 AU pre-perihelion on November 12, 2003. The CONTOUR Forward Imager (CFI), described in detail in this volume by Warren et al., has three filters designed for imaging in the coma emission bands of OH, CN and C_2 as well as filters designed to sample nearby dust continuum emissions (see Table I). Observations of coma emissions will begin about ten days before closest approach (CA) and continue until several seconds before CA. This will permit the sunward fan, as observed from Earth, to be mapped down to its source region on the nucleus. The coma images will also provide the context for the interpretation of the *in situ* mass spectrometer measurements.

Additional evidence for asymmetrical outgassing from cometary nuclei has come from recent HST observations using the Space Telescope Imaging Spectrograph, with $0.''025$ resolution along the slit (18 km for a comet at a geocentric distance of 1 AU). Observations of comets C/1995 O1 (Hale-Bopp) (Weaver et al., 1999), 103P/Hartley 2, and C/1999 H1 (Lee) all show that the OH emission is not centered at the same position as the optocenter of the dust coma (with the nucleus unresolved also at the optocenter). The magnitude of the offset is hundreds of km. While the interpretation that the observed asymmetry results from the superposition of OH derived from asymmetric outflow of water from the nucleus is in accord with the results

Table I. CFI Coma Filters.

Filter	Wavelength (Å)	FWHM (Å)	Transmission (%)
OH	3084	53	53
continuum	3453	76	54
CN	3874	76	90
C_2	5124	110	87
continuum	5247	54	85

from comet Encke described above, an icy grain halo, often postulated as a source of a large fraction of the water in the coma, cannot be ruled out with the data in hand. Such a halo would necessarily be composed of large grains so as to be able to survive at small heliocentric distances. CONTOUR imaging will be easily able to distinguish between these two mechanisms.

As noted above, a primary goal of the coma imaging investigation is to study coma structures. At the fast Encke approach speed of 28.2 km s^{-1}, the early coma images, at a range of 2.4×10^7 km, will have linear resolution in the coma similar to Earth-based observations and cover a rectangular area $\sim 1 \times 10^6$ km on a side. These should reveal the fan structure with half angle near 90° and set the context for the rest of the observations. By 1 day before encounter the fan structure should fill the frame (now 1×10^5 km on a side) with a resolution of 104 km $pixel^{-1}$ at the nucleus. If Sekanina's model holds, a highly collimated structure should become apparent in the inner coma pointing to the source region on the still unresolved nucleus. At this time, the spacecraft will be entering the coma just on the outside of the emission cone and, as the encounter progresses and the viewing geometry is modified, we can expect dramatic changes in the apparent distribution of emissions in the coma.

The CONTOUR pass through the central 50,000 km of the coma will occur in about 30 minutes, a time short compared with the approximate 15 hr rotation period of the nucleus (Fernández et al., 2000). At a range of 25,000 km, CFI will allow imaging at about 1 km $pixel^{-1}$ (The nucleus will be about 4 pixels across) while the 2.5° FOV covers distances out to about 500 km from the nucleus. The spacecraft's rapid pass to within a closest approach distance of about 130 km will allow imaging of the coma at a predicted SNR of the order of 10 along many lines of sight passing completely through the coma as well as lines of sight originating from within it. If the coma does not vary significantly over the 30 minute interval, this data set may allow inference of near-nucleus coma structures such as jets or shocks by a tomographic process, although the interpretation of structures in coma images may be complex

(Kitamura, 1990; Crifo et al., 1995). It may also be possible to associate coma structures with source regions on the nucleus.

A primary consideration for the short wavelength filters is the rejection of out-of-band continuum (mainly red) from cometary dust. Simulations of cometary spectra through the measured filter response curves indicates that for Encke the amount of long wavelength contamination through the OH filter (3090 Å) will be of the order of 1% or less. Fairly long exposures ($\sim$10 seconds) and on-chip binning (at some loss of spatial resolution) will be required to achieve our goal of a signal-to-noise ratio of 10 in this band.

4. Summary

Our current knowledge of the coma of Comet 2P/Encke makes this comet an ideal first target for the CONTOUR mission. The small amount of micron-sized dust particles and the known gas production rate allow for planning optimum observing sequences for both the imagers and the *in situ* instruments. In addition, the November 2003 apparition will be excellent for obtaining supporting ground and space-based observations which should provide a strong link of the CONTOUR measurements to the historical record.

Acknowledgements

This work was supported by the CONTOUR project through a sub-contract to Johns Hopkins University from Cornell University.

References

A'Hearn, M. F., P. V. Birch, P. D. Feldman, and R. L. Millis: 1985, 'Comet Encke – Gas production and lightcurve'. *Icarus* **64**, 1–10.

A'Hearn, M. F., R. L. Millis, D. G. Schleicher, D. J. Osip, and P. V. Birch: 1995, 'The ensemble properties of comets: Results from narrowband photometry of 85 comets, 1976-1992.'. *Icarus* **118**, 223–270.

A'Hearn, M. F., R. L. Millis, and D. T. Thompson: 1983, 'The disappearance of OH from Comet P/Encke'. *Icarus* **55**, 250–258.

A'Hearn, M. F. and D. G. Schleicher: 1988, 'Comet P/Encke's nongravitational force'. *Astrophys. J.* **331**, L47–L51.

Bertaux, J. L.: 1986, 'The UV bright spot of water vapor in comets'. *Astron. Astrophys.* **160**, L7–L10.

Bertaux, J. L., J. E. Blamont, and M. Festou: 1973, 'Interpretation of Hydrogen Lyman-Alpha Observations of Comets Bennett and Encke'. *Astron. Astrophys.* **25**, 415–430.

Budzien, S. A. and P. D. Feldman: 1991, 'OH prompt emission in Comet IRAS-Araki-Alcock (1983 VII)'. *Icarus* **90**, 308–318.

Budzien, S. A., M. C. Festou, and P. D. Feldman: 1994, 'Solar flux variability and the lifetimes of cometary H_2O and OH'. *Icarus* **107**, 164–188.

Code, A. D., T. E. Houck, and C. F. Lillie: 1972, 'Ultraviolet Observations of Comets'. In: *NASA SP-310: Scientific results from the orbiting astronomical observatory (OAO-2), edited by A. D. Code*. pp. 109–114.

Crifo, J. F., A. L. Itkin, and A. V. Rodionov: 1995, 'The Near-Nucleus Coma Formed by Interacting Dusty Gas Jets Effusing from a Cometary Nucleus: I'. *Icarus* **116**, 77–112.

Djorgovski, S. and H. Spinrad: 1985, 'Surface photometry of comet P/Encke'. *Astron. J.* **90**, 869–876.

Feldman, P. D., H. A. Weaver, and M. C. Festou: 1984, 'The ultraviolet spectrum of periodic Comet Encke (1980 XI)'. *Icarus* **60**, 455–463.

Fernández, Y. R., C. M. Lisse, H. Ulrich Käufl, S. B. Peschke, H. A. Weaver, M. F. A'Hearn, P. P. Lamy, T. A. Livengood, and T. Kostiuk: 2000, 'Physical Properties of the Nucleus of Comet 2P/Encke'. *Icarus* **147**, 145–160.

Festou, M. C.: 1981, 'The density distribution of neutral compounds in cometary atmospheres. I - Models and equations'. *Astron. Astrophys.* **95**, 69–79.

Festou, M. C. and O. Barale: 2000, 'The Asymmetric Coma of Comets. I. Asymmetric Outgassing from the Nucleus of Comet 2P/Encke'. *Astron. J.* **119**, 3119–3132.

Kitamura, Y.: 1990, 'A numerical study of the interaction between two cometary jets - A possibility of shock formation in cometary atmospheres'. *Icarus* **86**, 455–475.

Mäkinen, J. T. T., J. Silén, W. Schmidt, E. Kyrölä, T. Summanen, J.-L. Bertaux, E. Quémerais, and R. Lallement: 2001, 'Water Production of Comets 2P/Encke and 81P/Wild 2 Derived from SWAN Observations during the 1997 Apparition'. *Icarus* **152**, 268–274.

Raymond, J. C., M. Uzzo, Y.-K. Ko, S. Mancuso, R. Wu, L. Gardner, J. L. Kohl, B. Marsden, and P. L. Smith: 2002, 'Far-Ultraviolet Observations of Comet 2P/Encke at Perihelion'. *Astrophys. J.* **564**, 1054–1060.

Reach, W. T., M. V. Sykes, D. Lien, and J. K. Davies: 2000, 'The Formation of Encke Meteoroids and Dust Trail'. *Icarus* **148**, 80–94.

Sanzovo, G. C., A. A. de Almeida, A. Misra, R. Miguel Torres, D. C. Boice, and W. F. Huebner: 2001, 'Mass-loss rates, dust particle sizes, nuclear active areas and minimum nuclear radii of target comets for missions STARDUST and CONTOUR'. *Mon. Not. Roy. Astron. Soc.* **326**, 852–868.

Schleicher, D. G. and M. F. A'Hearn: 1988, 'The fluorescence of cometary OH'. *Astrophys. J.* **331**, 1058–1077.

Sekanina, Z.: 1988a, 'Outgassing asymmetry of periodic comet Encke. I - Apparitions 1924-1984'. *Astron. J.* **95**, 911–924.

Sekanina, Z.: 1988b, 'Outgassing asymmetry of periodic Comet Encke. II - Apparitions 1868-1918 and a study of the nucleus evolution'. *Astron. J.* **96**, 1455–1475.

Sekanina, Z.: 1991a, 'Cometary activity, discrete outgassing areas, and dust-jet formation'. In: *ASSL Vol. 167: IAU Colloq. 116: Comets in the post-Halley era*. pp. 769–823.

Sekanina, Z.: 1991b, 'Encke, the comet'. *J. Roy. Astron. Soc. Canada* **85**, 324–376.

Sekanina, Z. and H. E. Schuster: 1978, 'Dust from periodic comet Encke - Large grains in short supply'. *Astron. Astrophys.* **68**, 429–435.

Weaver, H. A., P. D. Feldman, M. F. A'Hearn, C. Arpigny, J. C. Brandt, and S. A. Stern: 1999, 'Post-Perihelion HST Observations of Comet Hale-Bopp (C/1995 O1)'. *Icarus* **141**, 1–12.

Whipple, F. L.: 1950, 'A comet model. I. The acceleration of Comet Encke'. *Astrophys. J.* **111**, 375–394.